

Landau-Zener-Stuckelberg interferometry of a single electron spin in a noisy environment

Pu Huang,¹ Jingwei Zhou,¹ Fang Fang,¹ Xi Kong,¹ Xiangkun Xu,¹ Chenyong Ju,^{1,*} and Jiangfeng Du^{1,†}

¹*Hefei National Laboratory for Physics Sciences at Microscale and Department of Modern Physics, University of Science and Technology of China, Hefei, 230026, China*

We demonstrate quantum coherent control of a single electron spin in a NV center in diamond using the Landau-Zener-Stuckelberg interferometry at room temperature. Interference pattern is observed oscillating as a function of microwave frequency. The decays in the visibility of the interference are well explained by numerical simulation which includes the thermal fluctuations of the nuclear bath which shows that Landau-Zener-Stuckelberg interferometry can be used for probing electron spin decoherence processes.

PACS numbers: 03.67.Ac, 42.50.Dv

Landau-Zener(LZ) tunneling is a well-known phenomenon associated with strong-driving. When a two-level system is driven through the avoided level crossing, LZ tunneling can be controlled to create various superposition of the energy eigenstates, like a coherent beam splitter. Combining two consecutive LZ tunneling leads to Landau-Zener-Stuckelberg(LZS) quantum interference which is analogous to the Mach-Zehnder(MZ) interferometry. LZS interference has been observed in Rydberg atoms[1, 2], quantum dots contacts[3], and recently in mesoscopic superconducting Josephson devices[4, 5], ultracold molecular[6] and Optical Lattices[7]. LZ tunneling and LZS interference have also been exploited for quantum states preparation[8, 9] and manipulation[10, 11]. Interaction with the environment disturbs the coherence of the quantum system and therefore manifests in the LZS interference pattern[12, 13]. LZS interferometry thus provides crucial information on the decoherence processes by the environments.

Single electron spins of nitrogen-vacancy centre(NV centre)has been one of the most popular candidate as a qubit carrier. The high controllability as well as a favorable coherence time promises room temperature quantum information processing[14–17]and high sensitive magnetometry[18–20]. High efficiency initialization of NV center spin on desired pure state can be done via optical pumping. Quantum coherent controls of individual spin can be realized using the conventional microwave pulsed controls. NV center is also an ideal platform for studying quantum phenomena, especially, the processes in a strong-driving regime such as anharmonic dynamics[21] and the multifrequency spectra[22].

In this letter, we carried out LZS interferometry on a NV centre in high purity diamond and demonstrated the feasibility of using LZS for quantum coherent control of single electron spin. In this experiment, we first realize a coherent beam splitter for electron spin states based on the LZ tunneling process, this is realized in and then, by repeating such process twice under different microwave frequency, quantum interference known as

Stuckelberg oscillation is observed. The decays in the interference fringes agrees well with numerical simulations taking into account the hyperfine coupling of the electron spin with the surrounding nuclear spin bath. Our study shows that the thermal fluctuations of the nuclear spins is the dominate cause of observed coherence lose at room temperature.

LZ tunneling was first studied by Landau and Zener[23, 24] and a description of the variety of phenomenon related to LZ tunneling and LZS interference can be found in a recent review[25]. The problem rely on a two-level system, described by the LZ Hamiltonian,

$$H_{LZ} = -\frac{\Delta}{2}\sigma_x - \frac{\varepsilon(t) - \varepsilon_0}{2}\sigma_z, \quad (1)$$

which contains a minimum energy separation Δ (the avoided level crossing), a time dependent driving field $\varepsilon(t)$ and a offset ε_0 . To implement LZ tunneling, the system is prepared in an eigenstate of σ_z , denoted by $|0\rangle$, while the driving field $\varepsilon(t)$ is set to be much larger than Δ . In this way the initial state $|0\rangle$ is close to one of the eigenstates of H_{LZ} . Next, $\varepsilon(t)$ is gradually tuned down, and as the system is swept through the avoided level crossing where $\varepsilon(t) = \varepsilon_0$, $|0\rangle$ undergoes LZ tunneling and is split into a superposition of $|0\rangle$ and $|1\rangle$. The probability of remaining in $|0\rangle$ is given by the well-known LZ formula:

$$P_T = \exp(-\frac{\pi}{2}\delta) \quad (2)$$

where $\delta = \Delta^2/v$ and v is the sweep velocity which equals to the value of $d\varepsilon(t)/dt$ at the avoided crossing. The LZS interferometer can also be conceived as a MZ interferometer, as shown in Fig. 1(b). Starting with $|0\rangle$, the system undergoes LZ tunneling at t_1 where the superposition of the $|0\rangle$ and $|1\rangle$ is generated. The system subsequently evolves and accumulates a relative phase θ_{12} . When $\varepsilon(t)$ is swept back to the avoided level crossing at t_2 , $|0\rangle$ and $|1\rangle$ interfere. The relative phase θ_{12} is given by

$$\theta_{12} = \int_{t_1}^{t_2} E_{01}(t)dt \quad (3)$$

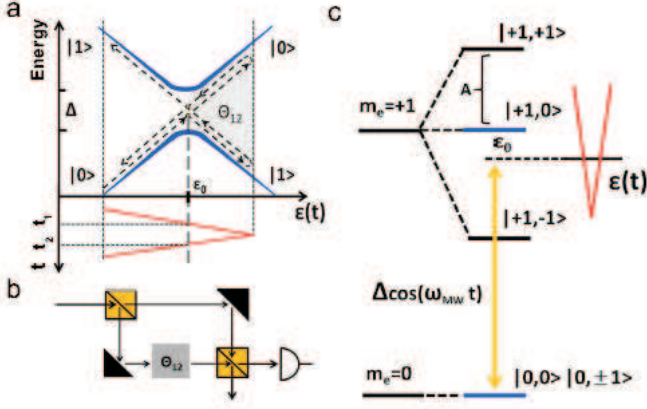


FIG. 1: (color online). Scheme for realizing an LZS interferometer on a single spin of the NV center in diamond. (a) Energy diagram of a two-level LZS interferometer: start at $|0\rangle$, the system is driven through the avoided crossing (at t_1) and split into a superposition of $|0\rangle$ and $|1\rangle$ via LZ tunneling; after accumulating a relative phase θ_{12} , $|0\rangle$ and $|1\rangle$ interfere at the avoided crossing (at t_2). (b) An MZ interferometer can be used to describe the LZS interferometer, with LZ tunneling acting as an optical beam splitter. (c) Realization of the LZS interferometer in an NV center: the two-level system of the LZS interferometer is expanded in electron states $m_e = 0$ and $m_e = +1$ with ^{14}N nuclear spin in the $m_I = 0$ state respectively (blue lines), a selective microwave field with frequency ω_{MW} (yellow double arrow) with strength Δ can act as the minimum energy separation after going into the rotating frame, ϵ_0 in the LZ problem can be tuned directly by the microwave frequency. The driving field $\epsilon(t)$ (red folded lines) is applied along $[111]$ crystal axis.

with $E_{01}(t)$ the energy difference between $|0\rangle$ and $|1\rangle$. It is θ_{12} that gives rise to the interference fringes in the occupation probability known as Stuckelberg oscillations.

The key issue in LZ tunneling is the realization of an avoided level crossing in energy states. Nevertheless, due to the large crystal splitting of the NV center, such a scheme cannot be implemented directly by electron spin resonance where a formidable strength of microwave field is required. In our scheme, the avoided level crossing is realized in the rotating frame where a microwave field can act as the minimum energy separation, similar method has been used in solid state electron spins [21, 22] as well as in superconducting Josephson devices [26]. We consider the NV center system which includes a spin-one electron spin and a nearby ^{14}N nuclear spin. The Hamiltonian can be written as

$$H_{NV} = DS_z^2 + g_e \mu_B B_z S_z + A_z I_z S_z. \quad (4)$$

Here $D \approx 2.87$ GHz is the crystal field splitting and B_z is the external magnetic field applied along the z axis ($[111]$ crystal axis) which lifts the degeneracy of electron spin states $|+1\rangle_e$ and $|-1\rangle_e$. μ_B is the Bohr magneton

and g_e the electron g -factor. The third term of Eq. (4) is the hyperfine coupling between the electron spin and the ^{14}N nuclear spin ($A \approx 2.18$ MHz), which contributes an effective field to the center spin conditioned on the ^{14}N state (we neglect the dynamics of ^{14}N for simplicity.) To realize the corresponding avoided level crossing in such a system, we first transform to the subspace spanned by $|0\rangle_e |0\rangle_I$ and $|+1\rangle_e |0\rangle_I$ as in Fig. 1(c), which will be denoted by $|0\rangle$ and $|1\rangle$ in the following. Applying a microwave field $\Delta \cos(\omega_{MW} t)$ along the x axis selectively excites the transition $|0\rangle \leftrightarrow |1\rangle$ when $\Delta \ll A$. In the rotating frame of ω_{MW} , Δ acts as a static field along the x axis. Finally, by assuming a time dependent field $\epsilon(t)$ along the z axis with amplitude smaller than A_z , the dynamics of $|0\rangle$ and $|1\rangle$ in the rotating frame can be expressed by H_{LZ} . By tuning the strength of the microwave field, one can change the minimum energy separation Δ , while by tuning the microwave frequency, ϵ_0 can be controlled.

We describe the experimental set-up for the demonstration of the LZS interferometry. The experiment is carried out on a home-built confocal microscope operated at room temperature. The sample is type IIa single crystal diamond with abundance of nitrogen electron spins less than 5 ppb. A single NV is addressed via a microscope mounted on a piezoscanner by its fluorescence signals. A Hanbury-Brown-Twiss setup with two photodetectors is used to ensure the single NV (data not shown). A 532 nm laser is used to initialize and read out the system. To manipulate the electron spin coherently, a microwave signal is first generated by a ratio signal generator, then a linear amplifier is employed to enhance the microwave power output. Finally, a $20 \mu\text{m}$ diameter copper wire terminated by a 50 Ohm resistance is used to radiate the microwave field to the NV center. The degeneracy between $|+1\rangle_e$ and $|-1\rangle_e$ is lifted by an external magnetic field generated by three pairs of Helmholtz coils, with resolution ≈ 0.01 Gauss. In the experiment a magnetic field of 5 Gauss is employed. The driving field $\epsilon(t)$ in H_{LZ} is generated by an Arbitrary Waveform Generator (AWG) and the signal is directly sent to the sample via the copper wire. In the experiment, the typical frequency of the driving field is several kHz which is much smaller than the microwave frequency, thus only the components along the z axis contribute. All signals are synchronized by a pulse generator. To build up statistic, we use typically 10^5 cycles in a single measurement. Δ is calculated using the output power of the amplifier and the amplitude of the driving field from the output voltage of the AWG. Typically, $\Delta \approx 500$ kHz at 20 dBm output while 4 V (peak-to-peak value of sine wave) in AWG corresponds to a driving field amplitude of 1.4 MHz.

Next, we describe the demonstration of the LZS interferometer. As preparation, we first accomplished LZ tunneling that can act as a beam splitter for electron spin states. Fig. 2 shows the measured and simulated LZ tun-

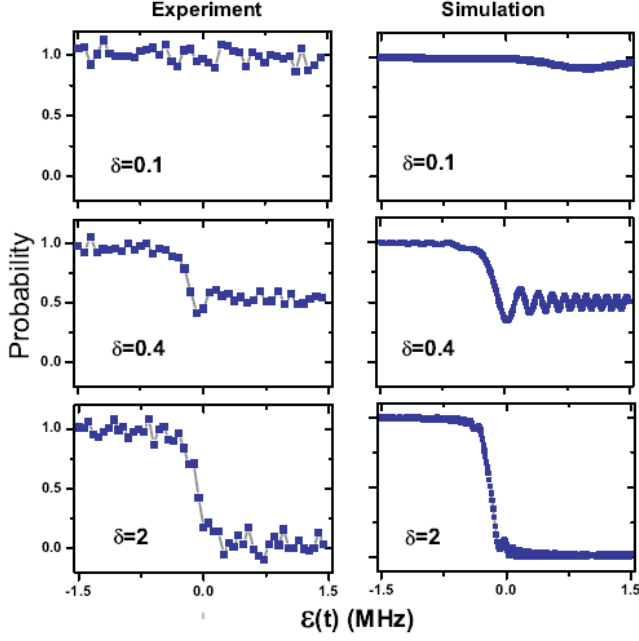


FIG. 2: (color online). Dynamics of the LZ tunneling. Measured(left) and simulated(right) dynamics of LZ tunneling under driving field: $\varepsilon(t) = \varepsilon \cos(2\pi w t)$ for different values of the adiabaticity parameter $\delta = \Delta^2/\varepsilon w$. To measure this curve, we set $\varepsilon = 1.5 \text{ MHz}$ and $\Delta = 0.11 \text{ KHz}$ and used different w . For the case $\delta \ll 1$, the system remains in $|0\rangle$ while for $\delta \gg 1$, the system evolves adiabatically with the driving field.

neling dynamics under a driving field $\varepsilon \cos(2\pi w t)$ for different values of the adiabaticity parameter $\delta = \Delta^2/\varepsilon w$. The simulation is based on H_{LZ} and the environment is not taken into account. By tuning the adiabaticity parameter, the tunneling probability can be controlled. Such a beam splitter can be further exploited to construct the LZS interferometer. According to the classical LZS interference theory[25], beginning in $|0\rangle$, the probability P of the system keeping in the same state after undergoing two consecutive LZ tunneling is given by

$$P = 4P_T(1 - P_T)\sin(\Phi)^2. \quad (5)$$

Here P_T is the LZ tunneling rate, and $\Phi = \Phi_S + \theta_{12}$ with Φ_S coming from Stokes phase. Fig. 3(a) shows the characteristic dynamics of the LZS interference process, while P_T as a function of sweeping velocity v is plotted in Fig. 3(b). To extract out the quantum coherence term in (4), we defined the interference visibility V as $V = P/4P_T(1 - P_T)$. Without noises, V is expected oscillating between 0 and 1 as a function of θ_{12} . However, as shown by the observed Stuckelberg oscillation(Fig. 3(b)), the visibility of interference fringes decrease as increasing the duration of the interference process. Such an effect clearly indicates a loss of quantum coherence between $|0\rangle$ and $|1\rangle$.

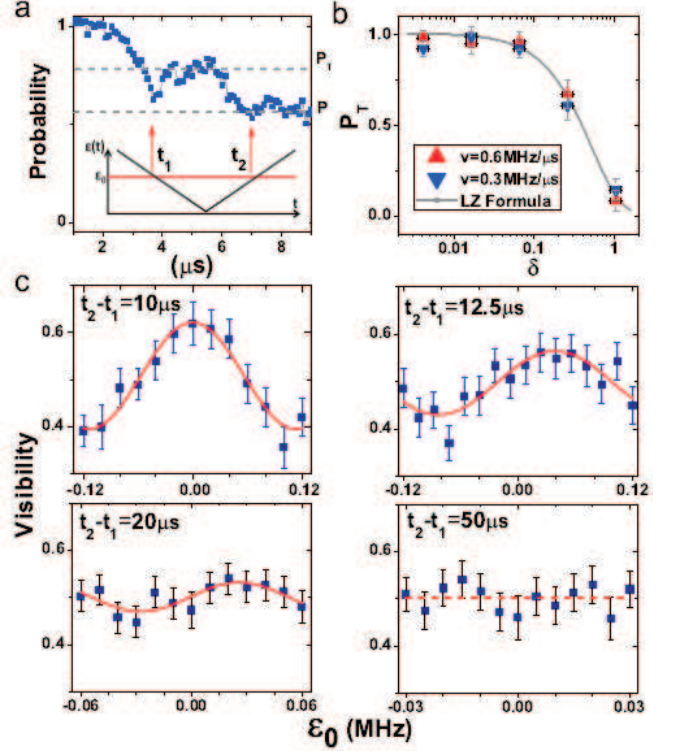


FIG. 3: (color online). LZS interferometer. (a) Dynamics of the LZS interference process driven by $\varepsilon(t) = vt$ (inset). gray lines indicate the probability of being in the state $|0\rangle$ after passing through the first (P_T) and the second avoided level crossing (P). (b) P_T as a function of the adiabaticity parameter δ (triangles) for different sweeping velocities. The result is in good agreement with the LZ formula (2). (c) Measured Stuckelberg oscillation curves (blue squares) for different evolution durations $t_2 - t_1$. The red line represents a fit to a cosine in order to obtain the visibility. The dashed line in last sub-diagram is a guide for the eyes since the visibility is nearly zero. In measuring this curve, we have adjusted the microwave power to bring P_T close to $1/2$, so that the oscillation amplitude is a maximum according to the classical LZ theory. The measured visibility is defined as $P/4P_T(1 - P_T)$.

To understand the observed decay in the interference pattern, the environment must be taken into account. In high purity single crystals, where the abundance of nitrogen electron spins is less than 5ppb, the main source of decoherence comes from the dipolar interaction with the ^{13}C nuclear spins [27]. This interaction, together with the dynamics of the nuclear spin bath can be expressed by $\hat{b}_z|1\rangle\langle 1| + H_{bath}$ in the subspace of the LZS interferometer. Here \hat{b}_z is the coupling to the nuclear spin bath, which can be written as $\sum_j \mathbf{A}_j \cdot \mathbf{I}_j$, with \mathbf{A}_j the coupling coefficient for the j th nuclear spin \mathbf{I}_j (the coupling strength is of the order of kHz). The fluctuation perpendicular is negligible since it is too weak to cause the spin-flip relaxation. H_{bath} contains the dynamics of the bath, which includes the Zeeman splitting (several kHz) of the

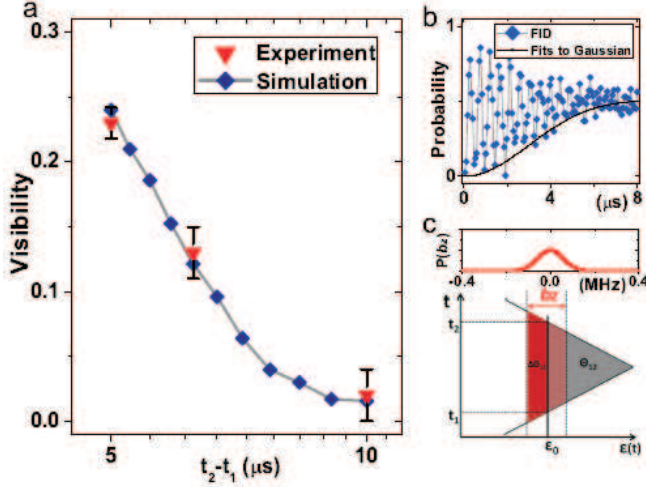


FIG. 4: (color online). Decoherence in the LZS process. (a) Measured (red triangles) and simulated (blue rectangle) visibility as a function of duration between the two LZ tunneling events. Agreement between theory and the experiment confirms that it is the thermal fluctuations of the nuclear spin bath that cause the decay of the visibility. (b) Measured FID signal, data is fitted to Gaussian decay (black line). (c) An intuitive picture can be employed to understand these observations. The fluctuations of nuclear spins produce an effective magnetic field b_z . It changes θ_{12} which is proportional to the area of the gray regime, with the result that the phase information is washed out.

nuclear spins in the external magnetic field and the dipolar interaction between nuclear spins (of the order of Hz). During the interference process, which occurs within tens of microsecond, the dynamics of the bath are negligible. We therefore expect that only the statistical fluctuations arising from the random orientations of the ^{13}C nuclear spins at room temperature contribute to the interference process. These fluctuations follow a Gaussian distribution $\exp(-b_z^2/2\beta^2)$ [28], where β can be directly extracted from the FID measurement (Fig. 4(b)). It is found that $\beta = 0.056\text{kHz}$ for the NV center under study.

Based on these considerations, numerical simulations were performed, with the measured and simulated results shown in Fig. 4(a). Good agreement between experiment and theory clearly establishes the decay mechanism as being due to nuclear spins. One also can capture the essence of the observations through the intuitive picture presented in Fig. 4(c). The phase giving rise to the interference fringes comes from the energy accumulated between two LZ tunneling points and is proportional to the duration of interference process multiplied by the amplitude of the driving field. The presence of the effective field b can change the position of the avoided level crossing and therefore cause fluctuations in θ_{12} . As a result, the oscillations are washed out and the visibility

decreases. This effect becomes more serious as the duration of the total process increases.

In conclusion, we have demonstrated a beam splitter of spin states of the NV centre at room temperature based on LZ tunneling. Our results showed that the tunneling probability is only given by the adiabaticity parameter δ which agrees with the original prediction of LZ formula. Combining two such beam splitters, LZS interferometer is realized and the Stuckelberg oscillation is observed, the decays in visibility of the interference fringes at room temperature is caused by thermal fluctuation of nuclear spins and agrees well with numerical simulations. Our work establishes the feasibility of using LZS interferometry for quantum coherent control and for probing decoherence processes of single spin in NV center.

We thank W. Yao and D. Culcer for helpful discussion and reading the paper. This work was supported by the National Natural Science Foundation of China (Grant No. 91021005), the CAS, and the National Fundamental Research Program (Grant No. 2007CB925200).

* cyju@ustc.edu.cn

† djf@ustc.edu.cn

- [1] S. Yoakum *et al.*, Phys. Rev. Lett. **69**, 1919 (1992).
- [2] Baruch, M.C and T.F. Gallagher, Phys. Rev. Lett. **68**, 3515 (1992).
- [3] Gorelik L.Y. *et al.*, Phys. Rev. Lett. **81**, 2538 (1998).
- [4] W. D. Oliver *et al.*, Science **310**, 1653 (2005).
- [5] S. Sillanpaa *et al.*, Phys. Rev. Lett. **96**, 187002 (2006).
- [6] M. Mark *et al.*, Phys. Rev. Lett. **99**, 113201 (2007).
- [7] S. Kling *et al.*, Phys. Rev. Lett. **105**, 215301 (2010).
- [8] D. J. Reilly *et al.*, Science **321**, 817 (2008).
- [9] H. Ribeiro *et al.*, Phys. Rev. Lett. **102**, 216802 (2009).
- [10] J. R. Petta *et al.*, Science **327**, 669 (2010).
- [11] Guozhu Sun *et al.*, Nature communications **1**(5), 51 (2010).
- [12] D. M. Berns *et al.*, Phys. Rev. Lett. **97**, 150502 (2006).
- [13] M. S. Rudner *et al.*, Phys. Rev. Lett. **101**, 190502 (2008).
- [14] M. V. Gurudev Dutt *et al.*, Science **316**, 1312 (2007).
- [15] P. Neumann *et al.*, Science **320**, 1326 (2008).
- [16] P. Neumann *et al.*, Science **329**, 542 (2010).
- [17] G. Balasubramanian *et al.*, Nat. Mater. **8**, 383 (2009).
- [18] J. R. Maze *et al.*, Nature **455**, 644 (2008).
- [19] G. Balasubramanian *et al.*, Nature (London) **455**, 648 (2008).
- [20] G. de Lange *et al.*, Phys. Rev. Lett. **106**, 080802 (2011).
- [21] G. D. Fuchs *et al.*, Science **326**, 1520 (2009).
- [22] L. Childress *et al.*, Phys. Rev. A **82**, 033839 (2010).
- [23] Landau, L.D., Phys. Z **2**, 46 (1932).
- [24] Zener, C, Proc. R. Soc. London A **137**, 696 (1932).
- [25] S. Shevchenko, S. Ashhab, and F. Nori, Phys. Rep. **492**, 1 (2010).
- [26] G. Sun *et al.*, arXiv:1010.5897.
- [27] L. Childress *et al.*, Science **314**, 281 (2006).
- [28] R. Hanson *et al.*, Science **320**, 352 (2008).